

<https://doi.org/10.1038/s42003-025-08235-0>

The genomics of the domestication syndrome in a songbird model species



Madza Farias-Virgens¹✉, David Peede^{2,3,4}, Terrence Deacon⁵, Kazuo Okanoya⁶,
Stephanie A. White^{7,8} & Emilia Huerta-Sanchez^{2,3,8}

Many domesticated animals share a syndromic phenotype marked by a suite of traits that include more variable patterns of coloration, reduced stress, aggression, and altered risk-taking and exploratory behaviors relative to their wild counterparts. Roughly 150 years after Darwin's pioneering insight into this phenomenon, reasonable progress has been made in understanding the evolutionary and biological basis of the so-called domesticated phenotype in mammals. However, the extent to which these processes are paralleled in non-mammalian domesticates is scant. Here, we address this knowledge gap by investigating the genetic basis of the domesticated phenotype in the Bengalese finch, a songbird frequently found in pet shops and a popular animal model in the study of learned vocal behaviors. Using whole-genome sequencing and population genomic approaches, we identify strain-specific selection signals in the Bengalese finch and its wild munia ancestor. Our findings suggest that, like in mammals, the evolution of the domestication syndrome in avian species involves a shift in the selective regime, capable of altering brain circuits favoring the dynamic modulation of motivation and reward sensitivity over augmented aggression and stress responses.

Stress and aggressive responses are significant traits of adaptive value for wild animals, manifested as impulsive reactions to perceived threats, often associated with high arousal states¹. Domesticated animals show lower levels of reactive aggression than their wild counterparts and more consistently exhibit risk-taking behaviors in contexts where they are highly motivated, following spontaneous learned associations and/or as reinforced by domestication practices². These changes are possible due to the attenuation of environmental sources of selection commonly found in the wild and often accompanied by selection associated with close socialization with individuals of the same or distinct species in the domestic setting³.

Here, we study one such domestication case in an under-examined order, the passerine lineage. Beginning ~250YBP, white-rumped munias (WRM; *Lonchura striata*), an extant wild songbird readily found throughout East Asia, were brought by aviculturists to Japan⁴. Shortly after the first century of domestication, these artificially bred munias started to exhibit piebald (i.e., patchy) patterns of plumage coloration, marking the origins of today's Bengalese finches (BF; *Lonchura striata domestica*)⁵ (Fig. 1A). Since then, Bengalese finches have become popular cage birds, known for their easy socialization and willingness to foster offspring, including those of other songbird species⁶. In addition to confirming Bengalese finches'

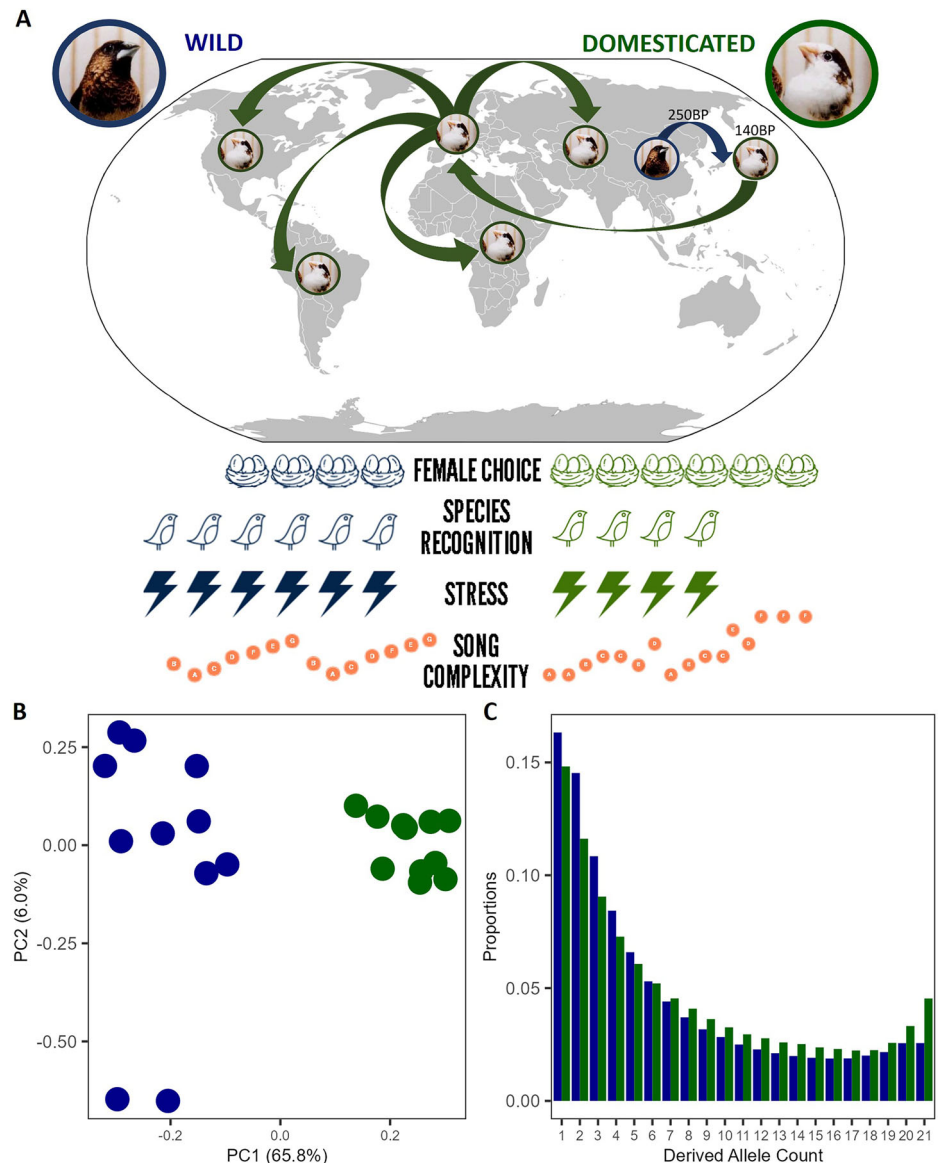
attenuated stress response, evidenced by decreased reactive aggression and neophobia relative to their munia ancestors^{7–9}, past research shows that adult Bengalese finches' song retains a greater degree of variability in the ordering of vocal elements than exhibited by their wild munia ancestors^{10,11}. These traits evolved in concert in the Bengalese finch, characterizing a prototypical case of the domestication syndrome in the avian clade.

While we have amassed considerable knowledge about the behavioral, physiological, and morphological differences between domesticated and wild mammals¹² and posed specific evolutionary hypotheses for how those changes came about^{13,14}, the extent to which this is paralleled in the non-mammalian realm is understudied. In this work, we address this gap in knowledge by investigating the genetic basis of the domesticated phenotype in the Bengalese finch. We hypothesized that, as observed in comparisons between other domesticated species and their wild counterparts¹⁵, the evolution of the domestication syndrome in the Bengalese finch likely involved the attenuation of selection associated with morphological and behavioral traits relating to stress and aggression and the intensification of ones related to reward aspects of social interactions and feeding. Using whole-genome sequencing data and population genomic approaches, we identified strain-specific and overlapping selection signals in the

¹Department of Biology, University of Washington, Seattle, WA, USA. ²Department of Ecology, Evolution, and Organismal and Evolutionary Biology, Brown University, Providence, RI, USA. ³Center for Computational Molecular Biology, Brown University, Providence, RI, USA. ⁴Institute at Brown for Environment and Society, Brown University, Providence, RI, USA. ⁵Department of Anthropology, University of California Berkeley, Berkeley, CA, USA. ⁶Graduate School of Arts and Sciences, The University of Tokyo, Tokyo, Japan. ⁷Department of Integrative Biology and Physiology, University of California Los Angeles, Los Angeles, CA, USA.

⁸These authors contributed equally: Stephanie A. White, Emilia Huerta-Sanchez. ✉e-mail: madzafv@gmail.com

Fig. 1 | Domestication drives behavioral and genomic divergence between Bengalese Finches and their wild ancestors, White-Rumped Munias. BF (right; domesticated; green) and WRM (left; wild; blue). **A** Environmental variables and their relationship to stress and birdsong complexity in wild and domesticated scenarios. **B** PCA of whole genomic genotype likelihoods in BF and WRM. **C** BF and WRM unfolded Site Frequency Spectra. Photo credits: Maki Ikebuchi (Bengalese finch and white-rumped munia photographs) and Wikimedia Commons (world map).



domesticated Bengalese finch and its wild munia ancestor and assessed the potential functional roles of annotated genes within the identified genomic regions of interest (ROIs). Consistent with our hypothesis, our findings suggest that selection signals in the munia population include genes of importance to hormonal regulation of stress and aggression. These selection signals are weaker or absent in the domesticated Bengalese finch, which instead shows evidence of selection on genes of relevance to dynamic modulation of motivation and reward sensitivity.

Results

Differentiation and variation along Bengalese finch and white-rumped munia genomes

The PCA of all Bengalese finch and white-rumped munia individuals shows a clear separation between the two populations along PC1 (Fig. 1B). This distinction is marked by a greater proportion of low-frequency genetic variants in the wild population, whereas variants at higher-to-fixed frequencies prevail in the domesticated (Fig. 1C). Differences in allelic frequencies between Bengalese finch and white-rumped munia are unevenly distributed across windows along individual chromosomes, allowing for the identification of local signals of differentiation between the two populations, as measured by *F_{st}*. While the genetic differentiation of windows within individual autosomes is close to the autosomal average, the sex chromosome

Z (ChrZ) shows considerably higher levels of differentiation (Table 1; Supp. Fig. 1). The higher differentiation of ChrZ may be partly attributed to this chromosome's smaller effective population size due to its heterogametic mode of transmission (males: ZZ; females: ZW)¹⁶. TajD values in munias varies less across their genome (autosomal TajD: var = 0.19; ChrZ TajD: var = 0.36), whereas in the domesticated, long stretches of the genome show either lower or higher TajD (autosomal TajD: var = 0.61; ChrZ TajD: var = 0.70) (Table 1; Supp. Fig. 1). Both tP and tW values are slightly lower across the genome in the Bengalese finch population than in the wild population, suggesting the Bengalese finch population has reduced overall genetic diversity in compared to the munia population (Table 1; Supp. Fig. 1). As with many domesticates, these genome-wide observations are likely due to the heightened effects of genetic drift, set off by the primary population bottleneck that marks the major domestication event¹⁷ and furthered by domestication practices of breeding small Bengalese finch populations in captivity.

Regions of interest (ROIs) in the Bengalese finch and the white-rumped munia genomes

Our *SweepFinder2* scans of the ZF aligned data allowed the detection of strain-specific signals in the domesticated Bengalese finch and its wild munia ancestor (Figs. 2 and 3; Supp. Fig. 2). We identified six ROIs exclusive

Table 1 | Summary of population genomics statistics across genomic regions

	Fst	TajD		tW				tP			
				BF		WRM		BF		WRM	
Autosomal	0.2±0.1 [0.1–0.4]	0.5±0.8 [-1.3–1.9]	0.3±0.4 [-0.6–1.1]	30.8±11.4 [10.0–55.6]	35.0±11.0 [9.8–57.3]	34.3±13.0 [9.5–61.7]	37.7±12.7 [9.5–63.3]				
ChrZ	0.3±0.1 [0.1–0.7]	0.4±0.8 [-1.3–1.8]	0.2±0.6 [-1.4–1.3]	19.7±9.6 [3.1–39.4]	23.4±10.1 [3.5–43.5]	22.5±12.1 [2.5–47.2]	24.9±11.8 [2.4–49.3]				
BF1-Chr1	0.4±0.1 [0.2–0.5]	-1.0±0.2 [-1.4–0.6]	0.4±0.4 [-0.7–1.1]	18.1±4.3 [8.6–26.4]	33.2±5.9 [24.5–48.0]	13.8±3.8 [6.6–21.2]	36.3±8.2 [21.8–55.3]				
BF2-Chr1	0.4±0.1 [0.3–0.5]	-1.2±0.3 [-1.9–0.6]	0.2±0.4 [-0.7–1.0]	15.6±4.9 [7.8–26.0]	28.6±6.7 [14.6–44.4]	10.9±3.7 [5.3–18.3]	30.1±7.6 [16.1–45.3]				
BF3-Chr1A	0.4±0.1 [0.3–0.5]	-1.7±0.5 [-2.5–1.0]	0.4±0.4 [-0.2–1.2]	19.8±10.1 [4.3–38.8]	42.3±10.6 [25.7–61.9]	11.5±6.2 [3.0–23.9]	47.0±12.6 [23.9–69.0]				
BF4-Chr2	0.4±0.1 [0.3–0.6]	-1.1±0.4 [-1.8–0.1]	0.0±0.4 [-0.8–0.8]	19.1±6.5 [9.8–33.6]	29.1±8.0 [13.5–45.5]	13.8±4.6 [7.2–22.8]	29.4±9.0 [12.8–50.0]				
BF5-Chr2	0.3±0.1 [0.1–0.5]	-0.6±0.8 [-1.5–0.9]	0.1±0.5 [-1.1–1.2]	24.6±21.3 [12.0–107.8]	37.0±20.0 [21.5–108.8]	21.5±20.2 [8.2–95.1]	37.1±14.8 [20.3–77.9]				
BF6-Chr4	0.4±0.1 [0.3–0.6]	-1.5±0.7 [-2.4–0.3]	0.3±0.5 [-0.6–1.3]	17.6±9.3 [0.5–32.4]	32.1±10.5 [5.8–49.9]	9.9±4.8 [0.4–18.3]	33.8±11.3 [7.9–53.5]				
BF7-Chr4	0.2±0.1 [0.0–0.4]	0.2±0.7 [-1.1–1.4]	-0.6±0.7 [-1.7–0.8]	5.9±3.5 [1.7–14.9]	10.2±5.3 [2.8–21.1]	6.4±4.3 [1.4–16.7]	8.9±5.5 [1.6–23.1]				
BF8-ChrZ	0.4±0.2 [0.1–0.8]	-0.3±0.8 [-1.4–1.6]	-0.1±0.9 [-1.8–1.5]	8.8±5.2 [1.7–19.0]	14.9±9.0 [1.7–33.4]	8.3±5.6 [1.1–20.7]	15.3±10.7 [1.2–39.4]				
WRM1-Chr1	0.2±0.1 [0.0–0.3]	0.4±0.7 [-1.0–1.5]	-0.3±0.7 [-1.5–1.1]	5.8±3.9 [1.0–17.5]	5.2±3.8 [0.7–19.3]	6.6±4.7 [0.4–15.2]	4.9±4.2 [0.5–14.5]				
WRM2-Chr1A	0.2±0.1 [0.1–0.3]	0.3±0.4 [-0.4–1.0]	-0.6±0.5 [-1.6–0.4]	10.6±3.0 [4.9–17.4]	8.0±3.3 [3.5–15.7]	11.5±3.5 [4.9–18.5]	6.9±3.2 [2.6–14.8]				
WRM3-Chr2	0.3±0.1 [0.0–0.5]	-0.3±0.8 [-1.8–1.0]	-0.4±0.6 [-1.3–0.7]	8.5±4.6 [1.5–15.9]	7.2±5.5 [1.6–20.5]	7.8±5.1 [1.0–14.6]	6.6±5.7 [1.4–18.7]				
WRM4-Chr3	0.1±0.0 [0.0–0.2]	-2.0±0.2 [-2.3–1.6]	-0.3±0.6 [-1.5–1.0]	36.5±6.3 [25.1–48.9]	5.8±2.2 [2.6–10.9]	18.9±3.5 [12.6–26.6]	5.4±2.6 [2.2–13.1]				

Values represent 10 kb windowed mean ± standard deviation [2.5%–97.5% quantile range].

BF Bengalese finch (domesticated), WRM white-rumped munia (wild).

to the domesticated population across four autosomes: BF1-Chr1, BF2-Chr1, BF3-Chr1A, BF4-Chr2, BF5-Chr2, BF6-Chr4 (Fig. 2; Supp. Figs. 15–26). Sweep signatures at regions overlapping BF2-Chr1 and BF6-Chr4 were additionally confirmed by *SweepFinder2* scans of the BF aligned data (Supp. Figs. 27–33). Genetic differentiation between Bengalese finches and munias in these regions exceeded that of 97% of autosomal windows (Table 1). In the Bengalese finch population, TajD values within each ROI were lower than 95% of autosomal windows, while in munias they were lower than 60%. Similarly, tW values were lower than 88% of autosomal windows in Bengalese finches and lower than 54% in munias, and tP values were lower than 95% in Bengalese finches and 56% in munias, consistent with a greater loss of variability in those genomic segments in the domesticated songbird (Table 1). These results suggest that these ROIs might have experienced recent or ongoing positive selection specific to the Bengalese finch population, resulting in higher differentiation from the ancestral munia population.

In the wild munia population, we identified four genomic ROIs encompassing sweep signals found in four autosomes (Fig. 3; Supp. Figs. 15–26). Among those, only one signal was exclusive to the munia population, WRM4-Chr3, whereas overlapping signals were detected in the domesticated population at WRM1-Chr1, WRM2-Chr1A, and WRM3-Chr2. The signals at regions WRM1-Chr1, WRM3-Chr2, and WRM4-Chr3 were additionally confirmed by *SweepFinder2* scans of the BF aligned data (Supp. Figs. 27–33). Overall, genetic differentiation in these ROIs was not markedly elevated compared to the rest of the autosomal genome, exceeding 53% of autosomal windows (Table 1). These results suggest that selective sweeps in these regions may have occurred in the ancestral munia population. Alternatively, these overlapping signals could be false positives, detected by *SweepFinder2* in both populations due to their shared demographic history.

Tajima's D values for windows overlapping ROIs WRM1-Chr1, WRM2-Chr1A, and WRM3-Chr2 were moderately lower in wild munias than in Bengalese finches, falling below 94% of autosomal windows in wild munias compared to 73% in Bengalese finches (Table 1). The WRM4-Chr3 ROI presented a different pattern of genetic variation, whereby the wild munia population showed an exclusive sweep signal but higher TajD values than the domesticated population. Closer inspection of the WRM4-Chr3 region reveals that TajD values in the Bengalese finch population trend lower as the scan enters the left end of the region, reaching max negative TajD ~ -2.0, and gradually reverse toward less negative values across this region. In contrast, TajD values in the wild munia population remain relatively stable and closer to 0 across WRM4-Chr3 (Fig. 3; Supp. Figs. 15–26).

At WRM4-Chr3, the decrease in Tajima's D in the domesticated Bengalese finch is accompanied by elevated tW values, higher than 72% of autosomal windows, and reduced tP values, lower than 89%, suggesting an accumulation of rare rather than common variants in this region (Table 1). In contrast, both tW and tP values in the wild munia are proportionally lower, each falling below 99% of autosomal windows (Table 1). This region is associated with a common fragile site prone to mutate and frequently undergoes large structural rearrangements in mammals and birds, within which breakpoints are located to the Parkinson's disease (PD) associated gene, *PRKN* [30]. Accordingly, our findings of greater variability in the Bengalese finch population at WRM4-Chr3 may relate to increased genomic instability at *PRKN* in the domesticated population.

As observed for the WRM1-Chr1, WRM2-Chr1A, and WRM3-Chr2 ROIs, overlapping sweep signals were detected in both the Bengalese finch and white-rumped munia populations at BF7-Chr4 (Fig. 3; Supp. Figs. 15–26), and additionally confirmed by *SweepFinder2* scans of the BF aligned data (Supp. Figs. 27–33). This region presented a unique pattern of genetic variation, whereby the Bengalese finch population showed a stronger sweep signal but higher TajD values than the munia population, greater than 29% of autosomal windows in Bengalese finches compared to 3% in white-backed munias (Table 1; Supp. Figs. 15–26). This pattern indicates that while both populations show signals of selection at BF7-Chr4, the Bengalese finch population might have experienced some form of balancing selection that has resulted in the retention of more intermediate alleles.

Sweep signals within ChrZ cover a broad genomic area, including a peak shared by both the domesticated and wild populations, BF8-ChrZ, flanked by regions showing increased CLR values only in the Bengalese finch (Supp. Figs. 15–26). The sweep signal in this region was additionally confirmed by *SweepFinder2* scans of the BF aligned data (Supp. Figs. 27–33). BF8-ChrZ shows a high degree of genetic differentiation between domesticated and wild populations, greater than 91% of ChrZ windows, alongside similarly negative Tajima's D values in both groups, lower than 80% and 72% of ChrZ windows, respectively (Table 1). These patterns suggest that while both populations have experienced a selective sweep, the specific alleles under selection might differ, leading to increased population divergence in this region.

The identified ROIs span several genes each (Supp. Table 2). As a next step, we surveyed the genes within each ROI to identify potential candidates that may account for the phenotypic distinctions observed between Bengalese finches and white-rumped munias (Table 2). Several of these genes exhibit selection signals common in domesticated avian and mammalian species, including various indigenous and selectively bred populations worldwide (Supp. Table 2). The results of this survey are discussed below.

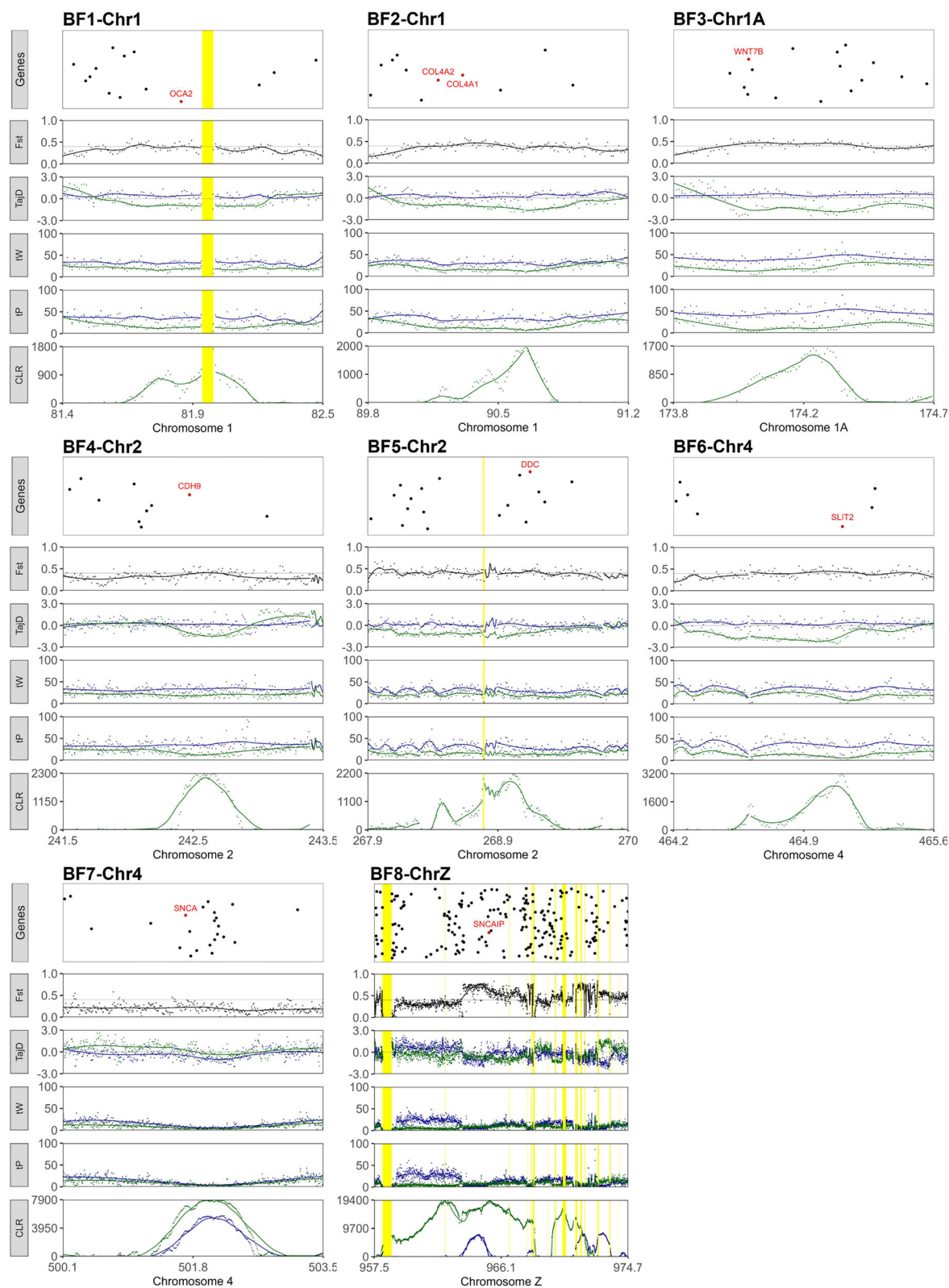


Fig. 2 | Genomic scans reveal putative domestication genes in Bengalese finches. BF (domesticated; green) and WRM (wild; blue). Each panel brings a schematic representation of the genes (midpoint) annotated within the defined ROI, with genes discussed in the main text highlighted and labeled in red; 10 kb window-based

measures of genetic differentiation (Fst) between BF and WRM populations, nucleotide diversity statistics (TajD, tW, and tP) for each BF and WBM populations; and CLR scores for a selective sweep for each BF and WBM populations. Yellow bars indicate gaps in the ZF reference genome. ROIs length is represented in Mb.

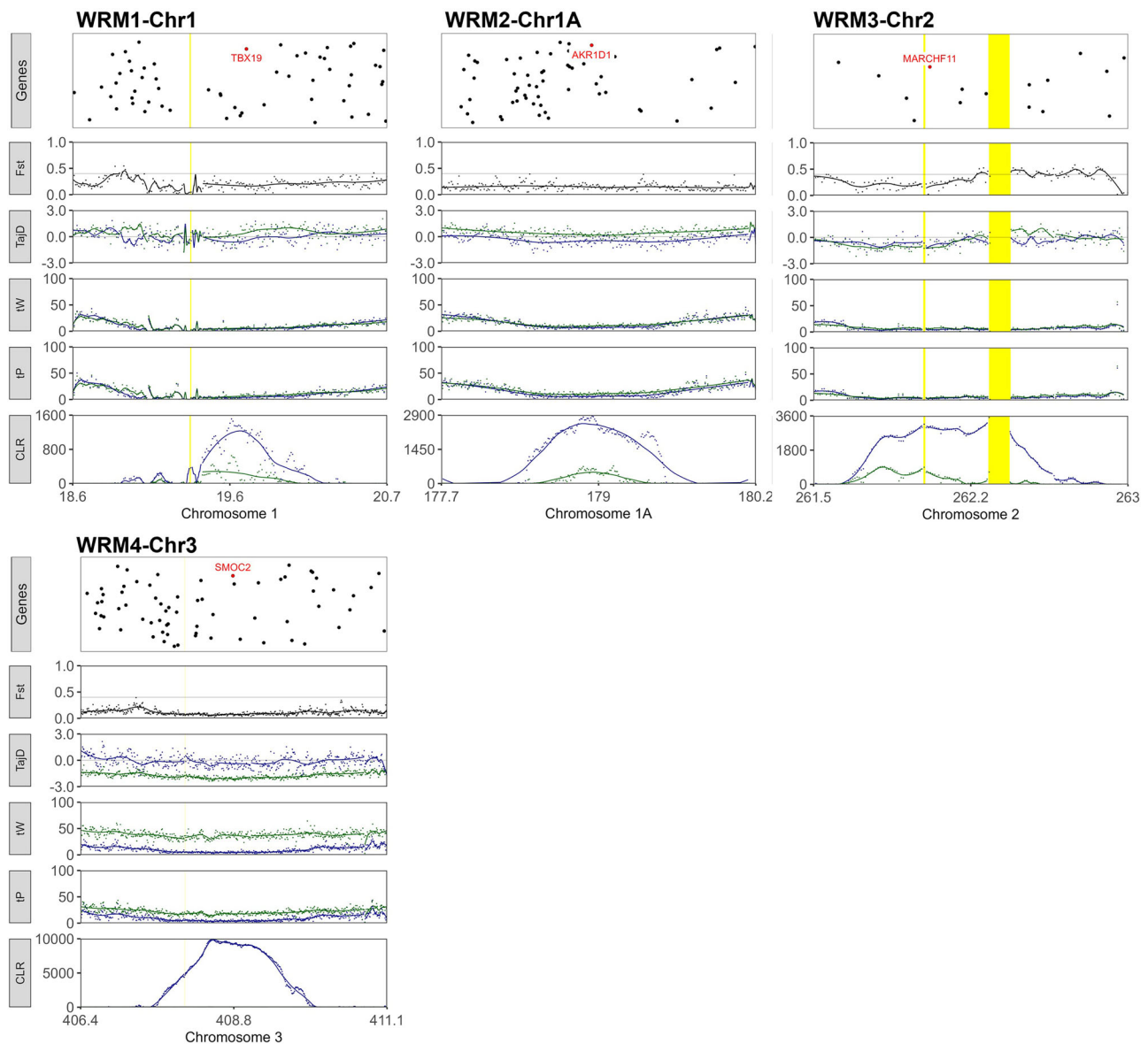


Fig. 3 | Wild-specific selection signatures in White-Rumped Munias. Plot structure and interpretation as in Fig. 2.

Discussion

Selection signals in the Bengalese finch population locate to regions of importance to color variation, neurodevelopment, and dopaminergic neuromodulation of behavior

Color variation in Bengalese finches. Eye and coat color tend to be fixed traits within wild species, with some variation related to age and sexual dichromatism¹⁸. In contrast, individual color variation in the adult stage is characteristic of many domestic species¹⁹. In line with this, plumage pigmentation is a noticeable difference between BFs and their munia ancestors. While white-rumped munias stereotypically have dark-brown heads, tails, and wing plumage, which transitions to more visibly barred feathers towards their flank and rump, Bengalese finches' plumage varies among individuals, comprising varied combinations of tones, with variable body distribution, including dark brown (chocolate), lighter brown (chestnut), yellowish brown tan (fawn), pale yellow (crémino) and white (albino) morphs. We found selection signals specific to the Bengalese finch at the *HERC2-OCA2* gene cluster in Chr1 (BF1-Chr1), with *OCA2* overlapping windows with the highest CLR values within this ROI. *OCA2* encodes the melanosomal transmembrane protein P, involved in the trafficking and processing of tyrosinase, a catalyzer of crucial steps in

the melanogenesis pathway, whose absence halts melanin production²⁰. *OCA2* expression is regulated by an element located within an intronic region of its contiguous upstream neighbor *HERC2*, where variants are major determinants of blue/brown iris coloration and are associated with differences in skin pigmentation in humans²¹. Mutations in *OCA2*'s mouse orthologue (i.e., the pink-eyed dilution locus), causing the lack of functional P protein, lead to a pink-eyed and light fur phenotype²⁰. Our per-gene summary statistics analysis reveals that all three genes exhibit considerably higher *Fst* values in intronic regions compared to exonic regions (Supp. Table 3). In the Bengalese finch population, these genes display consistently negative *TajD* values, with lower values in intronic regions relative to exonic regions. In contrast, the munia population shows consistently higher *TajD* values than the BF population, with less pronounced patterns differentiating intronic from exonic regions (Supp. Table 3). These aspects suggest that these genes' non-coding regulatory areas, rather than coding regions, may have been differentially affected during the divergence between Bengalese finches and the wild munia populations. Historical accounts indicate that piebald plumage coloration spontaneously emerged ~140YBP and was picked up by Japanese breeders, who further developed many Bengalese finch color morphs⁴.

Table 2 | Candidate genes for the domestication syndrome within ROIs

ROI	Sweep Signal		Genes	Gene product; function*
	BF	WRM		
BF1-Chr1			OCA2	P protein; melanogenesis ²⁰
BF2-Chr1			COL4A2, COL4A1	Collagen alpha-2 and alpha-1 (IV) chains; cell adhesion and signaling ⁶⁷
BF3-Chr1A			WNT7B	Protein Wnt-7b; neural crest specification and neural cell dendritic arborization ⁶⁸
BF4-Chr2			CDH9	Cadherin-9; synapse assembly ⁶⁹
BF5-Chr2			DDC	Dopa decarboxylase; dopamine biosynthesis ⁷⁰
BF6-Chr4			SLIT2	Slit homolog 2 protein: neural cell axon guidance ⁷¹
BF7-Chr4			SNCA	Alpha-synuclein; synaptic transmission ⁷²
BF8-ChrZ			SNCAIP	Alpha-synuclein interacting protein-1; synaptic transmission ⁷³
WRM1-Chr1			TBX19	T-box transcription factor TBX19; pituitary gland development ⁴⁴
WRM2-Chr1A			AKR1D1	Aldo-keto reductase family 1 member D1; steroid metabolism ⁷⁴
WRM3-Chr2			MARCHF11	E3 ubiquitin-protein ligase MARCHF11; cell differentiation ⁷⁵
WRM4-Chr3			SMOC2	SPARC-related modular calcium-binding protein 2; craniofacial morphology ⁵²

*Noted function of relevance for this study.
BF Bengalese finch (domesticated), WRM white-rumped munia (wild).

Noticeably, the Bengalese finch domestication was marked by significant breeding efforts for full white morphs, leading to the development of the black-eyed and pink-eyed albino strains⁴. Altogether, our findings raise the possibility of *HERC2-OCA2* gene cluster involvement in Bengalese finch plumage and eye coloration, which is especially relevant in the context of the development of the pink-eyed albino and other light-colored strains.

Increased flexibility in birdsong learning and practice. Several lines of evidence demonstrate Bengalese finches have evolved more complex vocal abilities than white-rumped munias: adult Bengalese finch song retains a greater degree of variability in the ordering of vocal elements than exhibited by munias¹¹; Bengalese finches exposed to multiple tutors compose their songs from a combination of excerpts from the different tutor's songs¹⁰; moreover, in cross-fostering experiments, Bengalese finches learn their white-rumped munia foster parent's song more efficiently than munias learn their Bengalese finch foster parent's song²².

Birdsong is regulated by dopaminergic innervation originating in the brain's motivational centers and projecting to specialized telencephalic nuclei, including the striatal region known as Area X and cortical vocal control nuclei, such as HVC (used as a proper name) and the robust nucleus of the arcopallium (RA) [58]. Our study found intensified selection in the Bengalese finch relative to their wild munia ancestors on regions comprising genes tightly linked to dopaminergic transmission, thus capable of affecting brain circuits highly relevant for song learning and production: *DDC* (BF5-Chr2), *SNCA* (BF7-Chr4), and *SNCAIP* (BF8-ChrZ), noting that *SNCAIP* is immediately adjacent to *LOC115491159*, the gene comprising windows with the highest CLR values within BF8-ChrZ. The regulation of dopamine (DA) levels within song nuclei relates to corresponding changes in the expression of enzymes involved in DA biosynthesis, like *DDC* (BF5-Chr2), coding for dopa decarboxylase²³. The gene *SNCA* (BF7-Chr4) negatively regulates DA availability within song control nuclei, where it is constitutively downregulated at both mRNA and protein levels^{24,25}. It has been proposed that overall low levels of alpha-synuclein in these regions may serve as a protective mechanism against protein aggregation and consequent motor deficits during aging²⁶. *SNCA* expression is developmentally downregulated during the critical period for song learning

within RA and Area X's adjacent efferent nucleus, the lateral magnocellular nucleus of the anterior nidopallium (LMAN)^{25,27}. In the adult songbird brain, alpha-synuclein is differentially regulated within Area X between vocal practice and performance, with increased levels scaling to the time spent singing alone for practice but not during singing directed to females²⁸. Though less is known about synphilin-1's function within the song circuit, *SNCAIP* (BF8-ChrZ) mRNA expression is significantly downregulated within Area X during song practice²⁹. This result is consistent with synphilin-1's role in regulating the ubiquitin-mediated degradation of alpha-synuclein³⁰ and suggests this interaction contributes to the modulation of song variability during practice.

Several of these genes exhibit considerably higher Fst values in intronic regions compared to exonic regions (Supp. Table 3). In the Bengalese finch population, these genes' TajD values are consistently negative and lower in intronic regions relative to exonic regions. In contrast, the wild munia population shows consistently higher TajD values, with less pronounced patterns distinguishing intronic from exonic regions (Supp. Table 3). An exception is *SNCA*, which exhibits a comparable degree of differentiation between intronic and exonic regions, with TajD values similarly negative in both the domesticated and wild songbird populations. Noticeably, *SNCA* is found in the ROI BF7-Chr4, where sweep signals overlap between Bengalese finches and white-rumped munias (Supp. Table 3).

Several genes located within the Bengalese finch ROIs exert a significant influence on the regulation of cell guidance and connectivity, particularly relevant in neurodevelopment, thus potentially contributing to differentiation and specialization of the song control circuit. These genes include: *COL4A2*, *COL4A1*, and *MYO16* (BF2-Chr1), *WNT7B*, *ATXN10*, and *FBLN1* (BF3-Chr1A), *CDH9* (BF4-Chr2), and *SLIT2* (BF6-Chr4), with *MYO16*, *FBLN1*, *CDH9*, and *SLIT2* overlapping windows with the highest CLR values within their respective ROIs. *COL4A2* gene product shows differential expression between the song nucleus HVC in male songbird brains and corresponding vestigial reminiscences in female brains in zebra finches, a species where song is sexually dimorphic³¹. *COL4A1* expression is particularly enriched in HVC, where it peaks during sensorimotor learning in zebra finches (i.e., 45 days post-hatch)³². Although less is known about the specific role of *SLIT2* within the song circuitry, the down-regulation of its paralog *SLIT1* in song nuclei RA and HVC and in the brainstem motor nucleus nXIIts is suggested to facilitate the targeting of ROBO-expressing

terminals and guide the development of neuronal projections from HVC to RA, as well as direct projections from RA to nXII, a connection critical for learned vocalizations³³.

Reduced neophobia in feeding contexts. Controlled observations reveal that Bengalese finches exhibit decreased levels of neophobia in feeding contexts relative to their wild counterparts, as demonstrated by their lower latency in approaching the food cup in the presence of a foreign object⁸. This result can also be explained by differences in food motivation between domesticated and wild, to which our discovery of evolutionary changes in regions encompassing genes implicated in reward aspects of food intake may relate. Changes in *SNCA* (BF7-Chr4) mRNA and protein levels are associated with reward aspects of social interactions in mammals^{34,35}. In vivo studies suggest that the *SNCA* gene product, alpha-synuclein, regulates DA availability in response to the direct action of metabolic hormones in DA centers or downstream from homeostatic signaling in the hypothalamus³⁵. Similarly, *SNCAIP* (BF8-ChrZ) gene product, synphilin-1, is implicated in food intake and fat deposition in mammals^{36–38} and in hyperphagia, first characterized in transgenic mice overexpressing this gene predominantly in neurons, which unexpectedly manifested obesity, and in the absence of PD-like symptoms³⁹. Signatures of selection at *SNCAIP* have been detected in broiler chicken lines divergently bred for abdominal fat content, which supports synphilin-1's relation to food intake and adiposity as being conserved in avian species⁴⁰.

Selection signals in the wild munia population are associated with hormonal regulation of stress and aggression

Like other domesticates, Bengalese finches exhibit less stress than their wild counterparts, as shown by lower levels of cortisol measured in fecal samples collected throughout the day, and lower reactive aggression, as demonstrated by less frequent biting responses when provoked with a stick attached to a piezo-electric sensor^{9,41}. In mammals and birds, stress and aggression are closely linked to hormonal regulation in the body, primarily mediated by cortisol, adrenaline, and testosterone⁴². As a result, genes associated with hormone function are likely to contribute to differences in stress and aggression between domesticated and wild animals⁴³. Guided by this rationale and previous genetic associations, we identified three genes related to hormonal regulation of stress and aggression within genomic regions showing selection signals exclusively in wild munias: *TBX19* (WRM1-Chr1), *AKR1D1* (WRM2-Chr1A), and *MARCHF11* (WRM3-Chr2). The gene *TBX19* (WRM1-Chr1) encodes a transcription factor that marks pituitary cell lines that will later express pro-opiomelanocortin (POMC), the peptide that elicits adrenocorticotrophic hormone (ACTH) release⁴⁴. Changes in *TBX19* are suggested to underlie tameness and timidity in Chinese indigenous pigs⁴⁵. Though *MARCHF11* (WRM3-Chr2) function in the pituitary remains unexplored, emerging findings suggest that its brain expression is regulated by social and stress-related cues tied to reproduction⁴⁶. *MARCHF11* expression is sexually dimorphic in midbrain vasopressin-responsive neurons, which are activated by prosocial stimuli (e.g., the presence of a female mouse, leading to mating or huddling) but not by antagonistic social stimuli (e.g., the sight of a male mouse, leading to fighting or drawing back)⁴⁶. In songbirds, neurons expressing the avian homolog of the mammalian vasopressin, vasotocin, exert effects on sex-specific behaviors, pair bonding, gregariousness, and aggression^{47,48}. These observations implicate *MARCHF11* in sex-specific reproductive physiology and behavior that discriminates between stress conditions, as regulated by vasopressin/vasotocin. Noticeably, the genomic region inclusive of *MARCHF11* shows high divergence in 11 *Lonchura* munia species radiated throughout Australia and Papua New Guinea⁴⁹; specifically, it shows high differentiation in two of four pairwise comparisons between sympatric *Lonchura* species with minimal genome-wide divergence, therefore possibly involved in generating adaptive diversity in munias in the wild. The gene *AKR1D1* (WRM2-Chr1A) falls within windows with the highest CLR values within its ROI. This gene encodes a steroid A-ring reductase, 5 β -reductase,

that is highly prevalent in the brain and pituitary of birds, where its primary function is to inactivate testosterone⁵⁰. In oscine species, steroid metabolism in the brain is linked to structural changes, particularly in the neural circuits that govern song production and modifications in sexual and aggressive behaviors⁵¹. Altogether, our findings indicate heightened selection on genes associated with the hypothalamic-pituitary-adrenal (HPA) axis function in white-rumped munias relative to their domesticated descendant, the Bengalese finches. This phenomenon may contribute to the observed differences in aggressive behavior and stress responses between these two groups, aligning with prior studies in mammalian domesticates¹⁵.

We also identified a selection signal exclusive to the wild munia population in a region of importance for craniofacial morphology, for which changes are associated with domestication in mammals^{52,53}. The sweep signal within WRM4-Chr3 ROI includes the gene *SMOC2*, which is immediately adjacent to *LOC115494389*, the gene having the highest CLR values within this ROI. *SMOC2* codes for a protein related to matrix assembly and cell adhesiveness, expressed in cartilage and bone during development and in the adult skeleton. In mammals, this gene product is implicated in craniofacial dysmorphism, specifically brachycephaly (i.e., shortening of the anteroposterior skull length and widening along the cranial mediolateral axis) and brachygnathism (i.e., underbite)^{52–54}. The role of *SMOC2* in craniofacial morphology appears to be conserved in birds, as it figures among genes showing significant SNP association with beak shape in Darwin finches⁵⁵. Though direct morphological comparisons between Bengalese finches and white-rumped munias are yet to be explored, the absence in the domesticated population of selective signals found in their munia ancestor at *SMOC2* could indicate craniofacial differences between the two. This finding is consistent with controlled observations that white-rumped munias show stronger biting to provocation than Bengalese finches⁹, as differences in beak dimensions and/or head width are the major predictors of bite force in finches⁵⁶. Differences in bite force between Bengalese finches and white-rumped munias, and possibly associated craniofacial allometric scaling, could derive from the lack of selection on traits such as physical endurance against aggression and foraging for harder and more varied materials and food in the wild.

Caveats and future directions

This study provides a foundation for understanding how specific genetic changes may underlie domestication-related traits in BFs, ultimately allowing for more targeted hypotheses and experimental approaches in future research. To build on our findings, further studies incorporating deeper sequencing efforts and broader population sampling are essential to refine our understanding of selection dynamics in Bengalese finches and white-rumped munias. A more extensive sequencing approach with larger and more diverse populations would provide a finer resolution of selection signals and allow for a more comprehensive assessment of genetic diversity across different lineages and geographic regions. Such efforts may help identify rare variants that contribute to traits expressed in the domesticated population. Additionally, results from our study could be leveraged to explore genotype-phenotype associations for the identified candidate genetic regions (e.g., in the context of controlled crosses between the wild and domesticated strains). Such associations could provide insights into how specific alleles might relate to domestication-related phenotypes differing between Bengalese finches and white-rumped munias, including variations in eye and plumage color, as well as behavioral traits like stress responses and aggression (e.g., biting reactions to stimuli).

Notably, our study found evidence of intensified selection in wild munias at genomic regions containing genes associated with stress and aggression, likely reflecting continued pressure to maintain these responses, which are critical for survival in natural environments. In contrast, the absence of similar signals in Bengalese finches may suggest a relaxation of selection in the domestic context, where such traits are less essential for fitness. To directly test this hypothesis, future analyses could compare dN/dS ratios and perform McDonald–Kreitman tests on fixed versus polymorphic sites to assess changes in selective constraint on stress-related genes

in the Bengalese finch lineage. Additionally, behavioral assays investigating the functional roles of these candidate genes in domesticated versus wild strains could yield valuable insights into how selection has contributed to observed differences in stress responses and aggression between them. These approaches would help differentiate between relaxed selection in the domestic form and alternative explanations, such as adaptive divergence in the wild lineage.

Conclusion

Results from various avenues of inquiry indicate that a typical path to domestication includes the attenuation of selection for augmented reactive aggression and the intensification of selection for dynamic modulation of motivation and reward sensitivity. Our findings suggest that the same principles apply to tame a songbird. Selective sweeps in the Bengalese finch comprise genes essential for DA synthesis, availability, and response in the songbird brain, thus highly relevant in the specialization and function of brain nuclei dedicated to song. Our scans also reveal selection signals specific to the Bengalese finch in genes linked to pigmentation differences in other animals, which could similarly explain its color morphs.

Methods

Sample collection

Blood samples were collected from 15 Bengalese finches and 15 white-rumped munia adult males housed in the Okanoya Lab at RIKEN-Brain Science Institute (RIKEN-BSI, Japan). Bengalese finch source colonies in the Okanoya lab originated from and are continuously supplied by various breeders in Japan and diligently maintained per standard bird breeder practices to avoid the undesired effects of inbreeding. Munias were imported from multiple wild colonies from different locations in Taiwan and bred in Okanoya Lab's aviaries, following similar practices as for Bengalese finches (~5 generations at the time of sample collection for this study). To avoid immediate relatedness biases, our samples from both the wild and domesticated populations included no first-order relatives. Samples were stored at -80°C at RIKEN-BSI until transported to UC Berkeley under a material transfer agreement and with USDA-APHIS approval (#128913). We have complied with all relevant ethical regulations for animal use and housing conditions, and all procedures were approved by RIKEN's Animal Care and Use Committee.

Whole-genome library preparation and sequencing

Total DNA was extracted from individual blood samples using a DNeasy kit (Qiagen, Germantown, MD) following protocols at the Evolutionary Genetics Laboratory at UC Berkeley. DNA quality was visually inspected by gel electrophoresis, and DNA concentrations were measured using NanoDrop spectrophotometry and a Qubit dsDNA BR Assay Kit (Thermo Fisher Scientific, Waltham, MA). Samples showing signs of degradation or yielding DNA concentrations insufficient for library preparation ($<50\text{ ng}/\mu\text{L}$) were discarded. Whole genomic double-stranded DNA from the remaining 13 Bengalese finch and 12 white-rumped munia DNA samples were fragmented to a 350 bp average size using a Bioruptor sonicator (Diagenode-Hologic, Denville, NJ). Sheared samples were visualized by gel electrophoresis to verify size distribution, and DNA concentrations were re-measured using a Qubit dsDNA BR Assay Kit. All 25 samples passed this quality-control step and were used to prepare whole-genome libraries using a KAPA Hyper Prep PCR-free Kit (Hoffmann-La Roche, Basel, Switzerland) and TruSeq adapters (Illumina, San Diego, CA). Library sizing information was obtained by electrophoresis using an Agilent 2100 Bioanalyzer system (Agilent Technologies, Santa Clara, CA). The 11 Bengalese finch and 11 white-rumped munia libraries passing this quality-control step were sequenced on 7 lanes in a 4000 HiSeq system (Illumina, San Diego, CA) in two replicates at UC Berkeley's QB3 sequencing facility.

Sequencing data preprocessing and quality control

The resulting paired-end sequencing reads (150 bp) underwent quality-control procedures using the software package *readcleaner* (github.com/

tplinderoth/ngsQC), which includes trimming adapters using *cutadapt* v1.10; pair-end read merging using *pear* v0.9.10; filtering contaminants identified through alignment to the human (GRCh38) and *E. coli* (ASM584v2) genomes using *bowtie2* v2.2.9⁵⁷, and generation of a final read quality report using *fastqc* v0.11.4⁵⁸ (Supp. Text 1).

Clean reads were aligned separately to the recently published, high-coverage zebra finch (ZF; *Taeniopygia guttata*) genome (bTae-Gut2.pat.W.v2: GCF_008822105.2) and the Bengalese finch genome (LonStrDom1: GCA_002197715) using the *Burrows-Wheeler Alignment* (BWA) tool. Genome indexes were generated for each reference genome using *BWA* v0.7.17⁵⁹ and *SAMtools* v1.0⁶⁰, along with sequence dictionaries from *Picard Tools* v2.0.1 (Picard Tools: CreateSequenceDictionary), and aligned using appropriate read group information (Supp. Text 1).

Duplicate reads were marked (Picard Tools: MarkDuplicates) in the ZF and BF aligned datasets, and an additional step of local indel realignment was performed using *GATK* v3.8.0⁶¹. Indels were called from all sampled individuals (GATK: HaplotypeCaller) and used to create lists of indel sites for each sampled individual separately (GATK: RealignerTargetCreator), which were then used as targets in the realignment (GATK: IndelRealigner) (Supp. Text 1).

A subsequent filtering step was applied to the ZF and BF aligned datasets to remove sites located in paralogous or repetitive sequence regions that confound short-read mapping using *ngsParalog* (github.com/tplinderoth/ngsParalog). This step involved calling single-nucleotide polymorphisms (SNPs) in each domesticated and wild population separately using *Analysis of Next Generation Sequencing Data* (ANGSD)⁶² (Supp. Text 1), a software package designed to handle low-coverage sequencing data by leveraging genotype likelihoods rather than called genotypes. The union of the identified variant positions (*angsd:-dovcf 1*) in each population served in estimating per-site paralog-log likelihood ratios. Likelihood ratios for each site were then compared between domesticated and wild, and the highest values for each site were retained. The cutoff above which a given site would be considered paralogous or repetitive and excluded from future analyses was calculated as defined in Supp. Text 2.

After excluding potential paralogous or repetitive regions, we calculated depth counts in the remainder positions for each individual in the ZF and BF aligned datasets (*angsd:-doCounts 1, -dumpCounts 2*) (Supp. Text 1). To avoid spurious results from missing data, sites covered in less than 9 out of 11 individuals in each population were further filtered from the data. Additionally, sites with average depth across individuals of $>20\times$ ($\sim 2\text{ SD} +$) in each population were filtered out, as they could be sequencing artifacts or represent paralogous and repetitive regions bypassed by the prior filtering. Finally, among the remaining sites, only diallelic sites were used in downstream analyses. After filtering, the sequencing data rendered an average per-site depth across chromosomes of 8x for both the ZF and BF aligned datasets (Supp. Table 1; additionally, a windowed analysis of average depth for the identified ROIs discussed below is presented in Supp. Figs. 3–14).

Population genomic analyses

Using the *GATK* model within *ANGSD*, we calculated genotype likelihoods and per-site allele frequencies for the ZF and BF aligned datasets (Supp. Text 1 and 2). Estimated per site allelic frequencies were used to estimate the Site Frequency Spectrum (1D-SFS) for each population as well as the 2-dimensional SFS (2D-SFS), with ancestral states as defined in each respective reference genome. To perform Principal Component Analysis (PCA) of the genetic relationship among individuals in our populations, we used a heuristic approach implemented in *PCAngsd* [22] (Supp. Text 1 and 2). Like *ANGSD*, *PCAngsd* is specifically designed for handling low-coverage sequencing data by considering genotype uncertainties instead of called genotypes.

A series of statistics summarizing the variation or distribution of alleles within the ZF aligned dataset was calculated using *ANGSD realsFS* (Supp. Text 1 and 2). In the analysis of multiple SNPs comprising genomic regions, *Fst* was calculated as the ratio of the sum of per site Bathia et al. estimations

of the variance *within* and *between* populations. This approach allowed us to calculate weighted *Fst* between our Bengalese finch and white-rumped populations in non-overlapping windows spanning 10 kb across the genome, as well as across all positions within a given gene's full-length and within exonic and intronic annotated boundaries (Supp. Data 1). Using *ANGSD realSFS saf2theta*, we calculated *Waterson's theta* (*tW*), *Pairwise theta* (*tP*), and *Tajima's D* (*TajD*)^{63,64} for each Bengalese finch and white-rumped population in the same genomic partitions (Supp. Data 2).

We performed selection scans using *SweepFinder2*⁶⁵ on the ZF aligned dataset, both implementations of a method that performs a composite likelihood ratio test for positive selection (Supp. Text 1). In this method, the likelihood of the null hypothesis is calculated for each population from their respective genome-wide 1D-SFS, and the likelihood of the alternative hypothesis is calculated from a model in which a recent selective sweep alters the neutral spectrum. *SweepFinder2* selection scans were run in non-overlapping windows spanning 10 kb each (Supp. Data 3). Subsequently, we defined genomic regions of interest (ROIs) as the contiguous segments containing the top 5% of windows with a higher composite likelihood ratio (CLR), as detected by *SweepFinder2* scans, in each domesticated and wild songbird population. Additionally, to characterize the gene content of ROIs originally identified using the ZF aligned dataset in the BF genome, we conducted *SweepFinder2* scans on both the BF and WRM data aligned to the BF genome. ROIs were defined using the same criteria as for the ZF aligned dataset, and overlapping ROIs identified in both approaches were compared (Supp. Table 4).

Statistics and reproducibility

Our analysis included a total of 11 BFs and 11, based on the number of per-breed/per-site individuals used in a previously published songbird study⁶⁶. We did not perform replication studies in additional, independent BF and WRM populations, primarily due to the difficulty of accessing both captive and wild WRM populations. All BF and WRM samples were processed in a single batch by the same bench experimenter, from total DNA extraction to whole-genome library preparation. To ensure blinding during these procedures, a second experimenter assigned anonymized labels (A[n]–Z[n]) to the BF and WRM samples. The correspondence between these anonymized labels and the original BF[n] and WRM[n] identifiers was only revealed after sequencing was complete.

Reporting summary

Further information on research design is available in the Nature Portfolio Reporting Summary linked to this article.

Data availability

The sequencing data (e.g., raw fastq files) generated during the current study are available in the SRA NCBI repository under BioProject accession code PRJNA1257907. The corresponding author can provide processed data generated as part of this study upon reasonable request.

Code availability

Custom code used to produce the main figures in the manuscript is available in the GitHub repository <https://github.com/madzafv/SongbirdDomesticationGenomics>.

Received: 3 September 2024; Accepted: 15 May 2025;

Published online: 03 June 2025

References

- Nimmo, D. G. et al. Animal movements in fire-prone landscapes. *Biol. Rev.* **94**, 981–998 (2019).
- Moretti, L., Hentrup, M., Kotrschal, K. & Range, F. The influence of relationships on neophobia and exploration in wolves and dogs. *Anim. Behav.* **107**, 159–173 (2015).
- Price, E. O. Behavioral development in animals undergoing domestication. *Appl. Anim. Behav. Sci.* **65**, 245–271 (1999).
- Svanberg, I. Towards a cultural history of the Bengalese Finch (*Lonchura domestica*). *Der Zoologische Gart.* **77**, 334–344 (2008).
- Okanoya, K. The Bengalese finch: a window on the behavioral neurobiology of birdsong syntax. *Ann. N. Y. Acad. Sci.* **1016**, 724–735 (2004).
- Dalrymple, P. The Society Finch: a wonderful worker. *AFA Watchb.* **25**, 43–43 (1998).
- Suzuki, K., Matsunaga, E., Yamada, H., Kobayashi, T. & Okanoya, K. Complex song development and stress hormone levels in the Bengalese Finch. *Avian Biol. Res.* **7**, 10–17 (2014).
- Suzuki, K., Ikebuchi, M., Kagawa, H., Koike, T. & Okanoya, K. Effects of domestication on neophobia: a comparison between the domesticated Bengalese finch (*Lonchura striata* var. *domestica*) and its wild ancestor, the white-rumped munia (*Lonchura striata*). *Behav. Process* **193**, 104502 (2021).
- Suzuki, K. & Okanoya, K. Domestication effects on aggressiveness: comparison of biting motivation and bite force between wild and domesticated finches. *Behav. Process* **193**, 104503 (2021).
- Takahasi, M., Yamada, H. & Okanoya, K. Statistical and prosodic cues for song segmentation learning by Bengalese Finches (*Lonchura striata* var. *domestica*). *Ethology* **116**, 481–489 (2010).
- Honda, E. & Okanoya, K. Acoustical and syntactical comparisons between songs of the white-backed munia (*Lonchura striata*) and its domesticated strain, the Bengalese finch (*Lonchura striata* var. *domestica*). *Zool. Sci.* **16**, 319–326 (1999).
- Sánchez-Villagra, M. *The Process of Animal Domestication*. (Princeton University Press, 2022).
- O'Rourke, T. et al. Capturing the effects of domestication on vocal learning complexity. *Trends Cogn. Sci.* <https://doi.org/10.1016/j.tics.2021.03.007> (2021).
- Wilkins, A. S., Wrangham, R. W. & Fitch, W. T. The “Domestication Syndrome” in mammals: a unified explanation based on neural crest cell behavior and genetics. *Genetics* **197**, 795–808 (2014).
- Hekman, J. P. et al. Anterior pituitary transcriptome suggests differences in ACTH release in tame and aggressive foxes. *G3 (Bethesda)* **8**, 859–873 (2018).
- Wang, Z. et al. Temporal genomic evolution of bird sex chromosomes. *BMC Evol. Biol.* **14**, 250 (2014).
- Lu, C. W., Yao, C. T. & Hung, C. M. Domestication obscures genomic estimates of population history. *Mol. Ecol.* **31**, 752–766 (2022).
- Negro, J. J., Carmen Blázquez, M. & Galván, I. Intraspecific eye color variability in birds and mammals: a recent evolutionary event exclusive to humans and domestic animals. *Front. Zool.* **14**, 53 (2017).
- Kowalski, E. & Bellone, R. Investigation of HERC2 and OCA2 SNP for iris color variation in Puerto Rican Paso Fino horses. *J. Equine Vet. Sci.* **5**, 319 (2011).
- Brilliant, M. H. The mouse p (pink-eyed dilution) and human P genes, oculocutaneous albinism type 2 (OCA2), and melanosomal pH. *Pigment Cell Res.* **14**, 86–93 (2001).
- Suarez, P., Baumer, K. & Hall, D. Further insight into the global variability of the OCA2-HERC2 locus for human pigmentation from multiallelic markers. *Sci. Rep.* **11**, 1–13 (2021).
- Takahasi, M. & Okanoya, K. Song learning in wild and domesticated strains of white-rumped munia, *Lonchura striata*, compared by cross-fostering procedures: domestication increases song variability by decreasing strain-specific bias. *Ethology* **116**, 396–405 (2010).
- Gale, S. D. & Perkel, D. J. Anatomy of a songbird basal ganglia circuit essential for vocal learning and plasticity. *J. Chem. Neuroanat.* **39**, 124–131 (2010).
- Kato, M. & Okanoya, K. Molecular characterization of the song control nucleus HVC in Bengalese finch brain. *Brain Res.* **1360**, 56–76 (2010).
- George, J. M., Jin, H., Woods, W. S. & Clayton, D. F. Characterization of a novel protein regulated during the critical period for song learning in the zebra finch. *Neuron* **15**, 361–372 (1995).

26. Nevue, A. A., Lovell, P. V., Wirthlin, M. & Mello, C. V. Molecular specializations of deep cortical layer analogs in songbirds. *Sci. Rep.* **10**, 18767 (2020).
27. Jin, H. & Clayton, D. F. Synelfin regulation during the critical period for song learning in normal and isolated juvenile zebra finches. *Neurobiol. Learn Mem.* **68**, 271–284 (1997).
28. So, L. Y., Munger, S. J. & Miller, J. E. Social context-dependent singing alters molecular markers of dopaminergic and glutamatergic signaling in finch basal ganglia Area X. *Behav. Brain Res.* **360**, 103–112 (2019).
29. Austin, A. T., Miller, J. E., Fraley, E. R., Horvath, S. & Stephanie, W. A. Molecular microcircuitry underlies functional specification in a basal ganglia circuit dedicated to vocal learning. *Neuron* **73**, 537–552 (2012).
30. Alvarez-Castelao, B. & Castano, J. G. Synphilin-1 inhibits alpha-synuclein degradation by the proteasome. *Cell Mol. Life Sci.* **68**, 2643–2654 (2011).
31. Lovell, P. V., Clayton, D. F., Replogle, K. L. & Mello, C. V. Birdsong “Transcriptomics”: neurochemical specializations of the oscine song system. *PLoS ONE* **3**, e3440 (2008).
32. Shi, Z. et al. Dynamic transcriptome landscape in the song nucleus HVC between juvenile and adult zebra finches. *Adv. Genet.* **2**, e10035 (2021).
33. Wang, R. et al. Convergent differential regulation of SLIT-ROBO axon guidance genes in the brains of vocal learners. *J. Comp. Neurol.* **523**, 892–906 (2015).
34. Smagin, D. A., Galyamina, A. G., Kovalenko, I. L. & Kudryavtseva, N. N. Altered expression of genes associated with major neurotransmitter systems in the reward-related brain regions of mice with positive fighting experience. *Int J. Mol. Sci.* **23**, 13644 (2022).
35. Cuvelier, E. et al. Overexpression of wild-type human alpha-synuclein causes metabolism abnormalities in Thy1-aSYN transgenic mice. *Front. Mol. Neurosci.* **11**, 321 (2018).
36. Emamgholi Begli, H., Vaez Torshizi, R., Masoudi, A. A., Ehsani, A. & Jensen, J. Genomic dissection and prediction of feed intake and residual feed intake traits using a longitudinal model in F2 chickens. *Animal* **12**, 1792–1798 (2018).
37. Li, H. et al. Genome-wide association studies for flesh color and intramuscular fat in (Duroc x Landrace x Large White) crossbred commercial pigs. *Genes* **13**, 2131 (2022).
38. Abied, A. et al. Genome divergence and dynamics in the thin-tailed desert sheep from Sudan. *Front. Genet.* **12**, 659507 (2021).
39. Li, X. et al. A novel obesity model: synphilin-1-induced hyperphagia and obesity in mice. *Int J. Obes.* **36**, 1215–1221 (2012).
40. Wang, T. et al. Analysis of selection signatures on the Z chromosome of bidirectional selection broiler lines for the assessment of abdominal fat content. *BMC Genom. Data* **22**, 18 (2021).
41. Suzuki, K., Yamada, H., Kobayashi, T. & Okanoya, K. Decreased fecal corticosterone levels due to domestication: a comparison between the white-backed munia (*Lonchura striata*) and its domesticated strain, the Bengalese finch (*Lonchura striata* var. *domestica*) with a suggestion for complex song evolution. *J. Exp. Zool. Part A Ecol. Genet. Physiol.* **317**, 561–570 (2012).
42. Lischinsky, J. E. & Lin, D. Neural mechanisms of aggression across species. *Nat. Neurosci.* **23**, 1317–1328 (2020).
43. Fallahsharoudi, A. et al. Domestication effects on stress induced steroid secretion and adrenal gene expression in chickens. *Sci. Rep.* **5**, 15345 (2015).
44. Liu, J. et al. Tbx19, a tissue-selective regulator of POMC gene expression. *Proc. Natl. Acad. Sci.* **98**, 8674–8679 (2001).
45. Wang, X. et al. Whole-genome sequence analysis reveals selection signatures for important economic traits in Xiang pigs. *Sci. Rep.* **12** <https://doi.org/10.1038/s41598-022-14686-w> (2022).
46. Patel, T. N. et al. Social interactions increase activation of vasopressin-responsive neurons in the dorsal raphe. *Neuroscience* **495**, 25–46 (2022).
47. Maney, D. L. & Goodson, J. L. Neurogenomic mechanisms of aggression in songbirds. *Adv. Genet.* **75**, 83–119 (2011).
48. Crino, O. L., Jensen, S. M., Buchanan, K. L. & Griffith, S. C. Evidence for condition mediated trade-offs between the HPA-and HPG-axes in the wild zebra finch. *Gen. Comp. Endocrinol.* **259**, 189–198 (2018).
49. Stryjewski, K. F. & Sorenson, M. D. Mosaic genome evolution in a recent and rapid avian radiation. *Nat. Ecol. Evol.* **1**, 1912–1922 (2017).
50. Schlinger, B. A. & Callard, G. V. A comparison of aromatase, 5α-, and 5β-reductase activities in the brain and pituitary of male and female quail (*C. c. japonica*). *J. Exp. Zool.* **242** <https://doi.org/10.1002/jez.1402420208> (1987/05/01).
51. Schlinger, B. A. Steroids in the Avian Brain: heterogeneity across space and time. *J. Ornithol.* **156**, 419–424 (2015).
52. Marchant, T. W. et al. Canine brachycephaly is associated with a retrotransposon-mediated missplicing of SMOC2. *Curr. Biol.* **27**, 1573–1584.e1576 (2017).
53. Bannasch, D. et al. Localization of canine brachycephaly using an across breed mapping approach. *PLoS ONE* **5**, e9632 (2010).
54. Quilez, J. et al. A selective sweep of >8 Mb on chromosome 26 in the Boxer genome. *BMC Genomics* **12**, 339 (2011).
55. Lawson, L. P. & Petren, K. The adaptive genomic landscape of beak morphology in Darwin’s finches. *Mol. Ecol.* **26**, 4978–4989 (2017).
56. Herrel, A., Podos, J., Huber, S. K. & Hendry, A. P. Evolution of bite force in Darwin’s finches: a key role for head width. *J. Evol. Biol.* **18**, 669–675 (2005).
57. Langmead, B. & Salzberg, S. L. Fast gapped-read alignment with Bowtie 2. *Nat. Methods* **9**, 357–359 (2012).
58. Kubikova, L. & Kostál, L. Dopaminergic system in birdsong learning and maintenance. *J. Chem. Neuroanat.* **39**, 112–123 (2010).
59. Li, H. & Durbin, R. Fast and accurate short read alignment with Burrows-Wheeler transform. *Bioinformatics* **25**, 1754–1760 (2009).
60. Li, H. et al. The sequence alignment/map format and SAMtools. *Bioinformatics* **25**, 2078–2079 (2009).
61. McKenna, A. et al. The Genome Analysis Toolkit: a MapReduce framework for analyzing next-generation DNA sequencing data. *Genome Res.* **20**, 1297–1303 (2010).
62. Korneliussen, T. S., Albrechtsen, A. & Nielsen, R. ANGSD: analysis of next generation sequencing data. *BMC Bioinforma.* **15**, 356 (2014).
63. Watterson, G. A. On the number of segregating sites in genetical models without recombination. *Theor. Popul Biol.* **7**, 256–276 (1975).
64. Tajima, F. Statistical method for testing the neutral mutation hypothesis by DNA polymorphism. *Genetics* **123**, 585–595 (1989).
65. DeGiorgio, M., Huber, C. D., Hubisz, M. J., Hellmann, I. & Nielsen, R. SweepFinder2: increased sensitivity, robustness and flexibility. *Bioinformatics* **32**, 1895–1897 (2016).
66. Salmón, P. et al. Continent-wide genomic signatures of adaptation to urbanisation in a songbird across Europe. *Nat. Commun.* **12** <https://doi.org/10.1038/s41467-021-23027-w> (2021).
67. Meuwissen, M. E. et al. The expanding phenotype of COL4A1 and COL4A2 mutations: clinical data on 13 newly identified families and a review of the literature. *Genet. Med.* **17**, 843–853 (2015).
68. Ji, Y., Hao, H., Reynolds, K., McMahon, M. & Zhou, C. J. Wnt signaling in neural crest ontogenesis and oncogenesis. *Cells* **8**, 1173 (2019).
69. Yamagata, M., Duan, X. & Sanes, J. R. Cadherins interact with synaptic organizers to promote synaptic differentiation. *Front. Mol. Neurosci.* **11**, 142 (2018).
70. Meiser, J., Weindl, D. & Hiller, K. Complexity of dopamine metabolism. *Cell Commun. Signal.* **11**, 34 (2013).
71. Bagri, A. et al. Slit proteins prevent midline crossing and determine the dorsoventral position of major axonal pathways in the mammalian forebrain. *Neuron* **33**, 233–248 (2002).
72. Siddiqui, I. J., Pervaiz, N. & Abbasi, A. A. The Parkinson Disease gene SNCA: evolutionary and structural insights with pathological implication. *Sci. Rep.* **6**, 24475 (2016).

73. Kruger, R. The role of synphilin-1 in synaptic function and protein degradation. *Cell Tissue Res.* **318**, 195–199 (2004).
74. Di Costanzo, L., Drury, J. E., Christianson, D. W. & Penning, T. M. Structure and catalytic mechanism of human steroid 5 β -reductase (AKR1D1). *Mol. Cell Endocrinol.* **301**, 191–198 (2009).
75. Morokuma, Y. et al. MARCH-XI, a novel transmembrane ubiquitin ligase implicated in ubiquitin-dependent protein sorting in developing spermatids. *J. Biol. Chem.* **282**, 24806–24815 (2007).

Acknowledgements

The authors acknowledge the funding sources that supported this work: MFV: Coordination for Improvement of Higher Education Personnel (CAPES), Brazil; NSF Bio Anthro DDRIG 1613709; Eureka and Hyde Fellowships—Department of Integrative Biology and Physiology, UCLA; Will Rogers Scholarship—Center for Accessible Education, UCLA; International Peace Scholarship—Philanthropic Educational Organization; and Summer Grant—Interdepartmental Program in Molecular, Cellular and Integrative Physiology, UCLA. SAW: UCLA Brain Research Institute William Scheibel Term Chair in Neuroscience. EHS: NIH-1R35GM128946; NSF-DEB 1557151; Brown Univ. and UC Merced start-up funds; and Alfred P Sloan Foundation Grant. DP: NIH-1R35GM128946 (to EHS) and Brown University Predoctoral Training Program in Biological Data Science (NIH T32 GM128596). The authors also thank the following individuals for their valuable contributions to this study: Maki Ikebuchi, PhD (Okanoya Lab—RIKEN Brain Science Institute); Lydia Smith, BSc (Evolutionary Genomics Laboratory—UC Berkeley); Tyler Linderoth, PhD (Integrative Biology—UC Berkeley); Yevgeniya Sosnovskaya, BA (Psychology and Anthropology—UC Berkeley); Anjana Krishnamurthy, BA (Integrative Biology—UC Berkeley); Parth Ingle, BSc (Computer Science and Engineering—UCLA); and Lalitha Balachandran, BA (Linguistics—UCLA).

Author contributions

Designed research: M.F.V., K.O., T.D.; performed research: M.F.V.; analyzed data: M.F.V., D.P., E.H.S.; contributed to writing: M.F.V., S.A.W., D.P., E.H.S., K.O., T.D.

Competing interests

The authors declare no known competing interests.

Additional information

Supplementary information The online version contains supplementary material available at <https://doi.org/10.1038/s42003-025-08235-0>.

Correspondence and requests for materials should be addressed to Madza Farias-Virgens.

Peer review information *Communications Biology* thanks the anonymous reviewers for their contribution to the peer review of this work. Primary handling editor: Jasmine Pan.

Reprints and permissions information is available at <http://www.nature.com/reprints>

Publisher's note Springer Nature remains neutral with regard to jurisdictional claims in published maps and institutional affiliations.

Open Access This article is licensed under a Creative Commons Attribution-NonCommercial-NoDerivatives 4.0 International License, which permits any non-commercial use, sharing, distribution and reproduction in any medium or format, as long as you give appropriate credit to the original author(s) and the source, provide a link to the Creative Commons licence, and indicate if you modified the licensed material. You do not have permission under this licence to share adapted material derived from this article or parts of it. The images or other third party material in this article are included in the article's Creative Commons licence, unless indicated otherwise in a credit line to the material. If material is not included in the article's Creative Commons licence and your intended use is not permitted by statutory regulation or exceeds the permitted use, you will need to obtain permission directly from the copyright holder. To view a copy of this licence, visit <http://creativecommons.org/licenses/by-nc-nd/4.0/>.

© The Author(s) 2025